Reentry vehicles: evaluation of plasma effects on RF propagation

TTC 2013
6th ESA International Workshop on Tracking, Telemetry
and Command Systems for Space Applications ESA-ESOC, 10 - 13 September 2013

REENTRY VECHICLES: EVALUATION OF PLASMA EFFECTS ON RF PROPAGATION

G.Vecchi[1], F.Vipiana[2], J.Tobon Vasquez[3], M.Visintin[4], F.Milani[5] , M.Bandinelli[6], M.Sabbadini[7].

[1]*Politecnico di Torino, Corso Duca degli Abruzzi, 24, 10129 Turin, Italy. Email: giuseppe.vecchi@polito.it*
[2]*ISMB Istituto Superiore Mario Boella, Via Pier Carlo Boggio, 61, 10138 Turin, Italy. Email: vipiana@ismb.it*
[3]*ISMB Istituto Superiore Mario Boella, Via Pier Carlo Boggio, 61, 10138 Turin, Italy. Email: tobonjorge@gmail.com*
[4] *Politecnico di Torino, Corso Duca degli Abruzzi, 24, 10129 Turin, Italy. Email: monica.visintin@polito.it*
[5]*IDS Ingegneria Dei Sistemi, Via Flaminia 1068, 00189 Rome, Italy. Email: f.milani@idscorportaion.com*
[6]*IDS Ingegneria Dei Sistemi, Via Enrica Calabresi 24, 56121 Pisa, Italy. Email:m.bandinelli@idscorporation.com*
[7]*ESA/ESTEC, P.O. Box 299, AG Noordwijk ZH, The Netherlands. Email: Marco.Sabbadini@esa.int*

I. INTRODUCTION

In the frame of communication technology relevant to re-entry vehicles, the communication black-out occurring in the presence of plasma is one of the main challenging issues.

The re-entry plasma is a complex physical system, where the ionization derives from a shock-wave and non-equilibrium phenomena. As discussed elsewhere, the time scales of plasma dynamics (including its evolution along mission trajectory) and radio wave propagation are well separated so that radio wave propagation can be solved at an appropriate number of time "snapshots" in which plasma dynamics is held unchanged and considered as known.

In this activity, a consistent effort has been devoted to model the electromagnetic issues related to radiofrequency propagation from/to antennae installed aboard the vehicle to the ground stations/Data Relay Satellites. For the involved range of operative frequencies and expected densities, the plasma can be considered as an inhomogeneous dielectric, working both in the propagation and cut-off regions. The associated electromagnetic problem is solved in two steps, via use of the field equivalence principle. The vehicle-plasma system is substituted by equivalent (Love's) currents on its boundary, radiating in free space; the fields on the boundary are obtained by solving the propagation problem from the antenna, installed on the spacecraft, up to the plasma boundary, through the Eikonal approximation.

Unlike other well-known numerical methods (e.g. FEM), this technique is not intrinsically limited by the electrical dimension of the vehicle-plasma system. This enables to analyze high frequency problems.

Since the formation of the re-entry plasma critically depends on the re-entry vehicle shape and kinematics, the related model has been directly derived from the output data of the Computational Fluid Dynamics simulations.

All the results of the above mentioned activities have been collected in a new software, the AIPT (Antenna In Plasma Tool, integrated into ADF-EMS, Antenna Design Framework Electromagnetic Satellite) able to predict the electromagnetic propagation in the presence of the plasma.

The AIPT in cooperation with the DLBS (Dynamic Link Budget Simulator) can determine both the BER (Bit Error Rate) and FER (Frame Error Rate) of the received signal.

II. ANALYSIS OF RF PROPAGATION

In order to evaluate the plasma effects on the RF propagation, two groups of analysis have been carried out:

- Analyses in the free space condition
- Analyses in the presence of plasma

By comparing the output of the two groups of analyses, the plasma effects can be determined.

To perform the analyses, a set of scenarios have been set up, each one being defined by:

- The vehicle type
- The mission (i.e. reentry trajectory)
- The placement of the antennae aboard the spacecraft
- The definition of the ground stations or DRS, Data Relay Satellites
- The communication architecture

All of the addressed aspects can be customized according to the specific analysis goal.

A. Reentry vehicles platform model

In the free space case the analyses have been carried out through a MoM (Method of Moments) solver, while in the presence of plasma a 3D Ray Tracer solver has been used. Thus, the e.m. (electromagnetic) model of the platform has been built accordingly to the involved solver.

In the free space case the platform is represented by a triangle based meshed model, with a sampling of about λ/10. The MoM platform CAD models have been rebuilt from the CFD (Computational Fluid Dynamics) data, in order to ensure coherence on the geometry data between the free space and the cases with plasma. Doing so, the antenna positioning data are valid for both cases.

B. Missions

All the addressed scenarios represent vehicles reentering from either the ISS (International Space Station) or the Moon. Two types of vehicles have been involved in the analyses: a lift-guided capsule (ARD-like, Atmospheric Re-entry vehicle Demonstrator) and a lifting body (IXV-like, Intermediate eXperimental Vehicle).

The analyzed missions are here below reported:

- IXV-like vehicle re-entry from ISS and from the Moon
- ARD-like vehicle re-entry from ISS and from the Moon
- ARD-like vehicle re-entry from LEO (Low Earth Orbit)

The trajectories are defined as a list of position and attitude samples.

C. Ground Station

Two link options have been selected for the analyses:

- Direct link, using ground stations located on either islands or ships. Their position have been determined through an optimized visibility analysis based on both the ground stations visibility mask and the beam extension of the antennae installed aboard the reentry vehicle.
- Indirect link, via a Data Relay Satellite located at a given position.

Eliminato: which basis

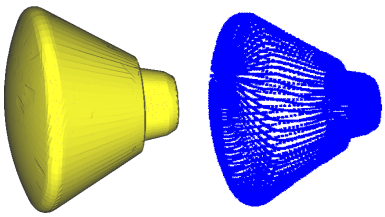

Fig. 1. MoM/CFD models of ARD platform

Tab. 1. Ships and DRS position

Mission	Latitude North [deg]	Longitude East [deg]	Altitude [km]
ARD from ISS	3.500	-161.700	0.01
	3.900	-155.000	0.01
	3.800	-150.000	0.01
	3.600	-145.000	0.01
	3.580	-141.500	0.01
IXV from MOON	-6.500	-179.800	0.01
	-2.000	-173.000	0.01
	-3.000	-170.500	0.01
	-3.000	-169.200	0.01
DRS	0	-174	35786

D. Plasma model and RF propagation

For the involved ranges of frequency and density, and because of the negligible intensity of the (Earth) magnetic field, for RF propagation the plasma is modeled as an inhomogeneous dielectric whose complex (relative) permittivity is expressed by Equation (1):

$$\varepsilon(x,y,z;f) = n^2(x,y,z;f) = 1 + \frac{f_p^2(x,y,z)}{f(jf_c^2(x,y,z) - f)} \tag{1}$$

where f is the link frequency, f_p and f_c are the electron plasma frequencies (related to the electron number density) and the collision plasma frequency (essentially related to the temperature) respectively.

The modeling is based on the equivalence theorem; the entire region containing the vehicle and the possible plasma cloud is delimited by an equivalence surface, lying where the plasma can be considered absent, or such that its effects on RF wave propagation can be totally neglected .

The fields to the exterior of this region are represented exactly by the radiation of the equivalent currents derived from the fields at the equivalence surface. Rather than solving Maxwell equations without any approximation, in this region we apply the so-called Eikonal approximation ("Ansatz"), represented by the so-called Lunemburg-Kline series for the fields **Errore. L'origine riferimento non è stata trovata.**

Eliminato: [1].

In the first order of Lunenburg - Kline series approximation, the fields are being expressed through (2):

$$\begin{aligned} E(r) &\approx E_0(r)\exp(-jk_0S(r)) \\ H(r) &\approx H_0(r)\exp(-jk_0S(r)) \end{aligned} \tag{2}$$

where E_0, H_0 and S are assumed to be slowly varying over one (local) wavelength $\lambda = \lambda_0/n$. This translates into the same requirement for the medium parameters, that in turn can be stated as the condition:

$$\lambda\nabla|\log(n)| << 1 \tag{3}$$

Of course this translates into a smoothness hypothesis on the shape of plasma density profiles, at least in the region of interest for radiation. In addition, however, note that ray-tracing is known to be very "robust" and to yield meaningful results, yet with lower accuracy, also when its starting Ansatz is not well verified.

Isolated points or loci where the Eikonal Ansatz is invalid will be called "critical points" in the following.

Insertion of Lunenburg - Kline approximation into Maxwell equations, together with the slow–variation assumption, yield the Eikonal equation:

$$\nabla|S| = n \tag{4}$$

for the Eikonal normalized phase S whose solution, upon specification of an initial phase front, provides the ray trajectories. In other words, the numerical solution of the Eikonal equation is formulated in terms of equations for the characteristic curves, involving the normalized local wavevector ξ :

$$\xi = \nabla|S| \tag{5}$$

and the position x along the ray itself. Using the arc-length s along the ray, the characteristics method results in solving the following system of ordinary differential equations (ODE):

$$\begin{cases} \dfrac{\partial x_i}{\partial s} = \dfrac{1}{n}\xi_i \\ \dfrac{\partial \xi_i}{\partial s} = \dfrac{\partial n}{\partial x_i} \end{cases} \tag{6}$$

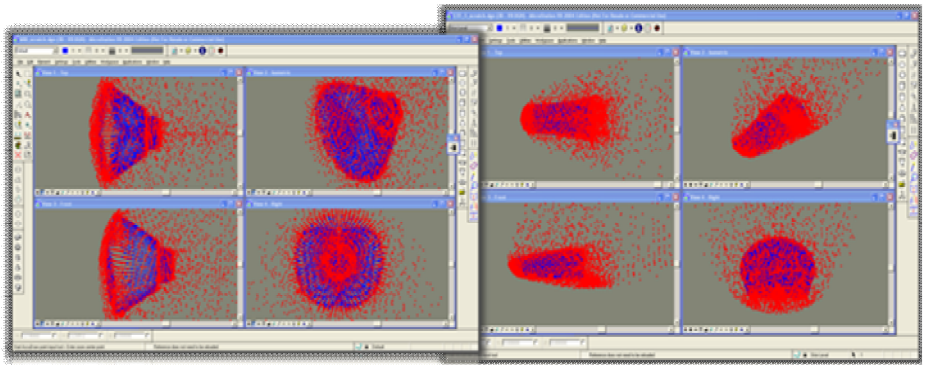

Fig. 2. Plasma and reentry vehicle CFD models

The equation above provided the position vector x and the Eikonal phase function *S* that is obtained by a line integral over the characteristic curve (potential recovery):

$$S(x(s)) = \int_0^s \xi(x) \cdot dl \tag{7}$$

The field amplitudes can be found along rays by using the relationship:

$$|E_0|(s_2) = \left| \frac{\rho_1 \rho_2}{(\rho_1 + \xi_2 - \xi_1)(\rho_2 + \xi_2 - \xi_1)} \right| |E_0|(s_1) \tag{8}$$

where ρ_1 and ρ_2 are the two radii of curvature of the wave front at s_1.

E. Spacecraft antennae model

A LHC (Left Handed Circular) polarized aperture-coupled patch antenna, operating in the S band, has been installed aboard both reentry vehicle types at given locations. The carrier frequency has been set to 2.26GHz . Antennae have been at first analyzed as stand-alone units; afterwards they've been converted into equivalent sources and mounted on the platform at specific and customizable locations, as reported in Tab. 2.

Fig. 3 shows the radiation pattern of the mounted antennae, in the absence of the plasma.

Formattato: Corpo del testo, Allineato a sinistra

Eliminato: Fig. 3

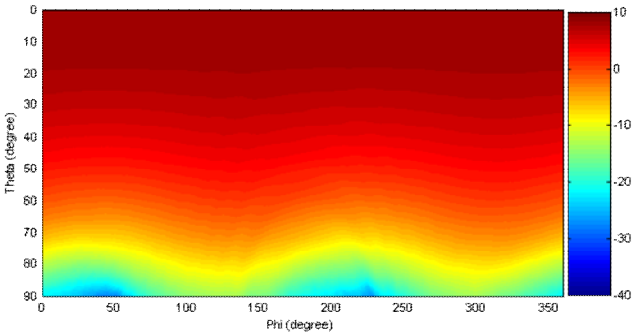

Fig. 3. LHCP gain map at 2.26GHz

Tab. 2. Antennae mounting points

Vehicle type	Installation vehicle side in the body reference frame	Antenna x coordinate	Antenna y coordinate	Antenna z coordinate
IXV	+Y	3.067	0.913	0
	-Y	3.067	-0.913	0
	+Z	3.52	0	0.783
ARD	+Y	1.081	0.998	0
	-Y	1.081	-0.998	0
	+Z	1.081	0.005	0.998
	-Z	1.081	0.005	0.998

F. Communication system

The telemetry bit rate is set equal to 192 kbit/s and 100 kbit/s for for IXV-like and ARD-like vehicles, respectively; the tele-command bit rates are 72 kbit/s and 8 kbit/s; it is in fact assumed that voice channels are present in the IXV case. The figures G/T are set equal to 13.5 dB/K for the ground station and -18 dB/K for the vehicle; the antenna gains are 35 dBi for the ground station and 8.5 dBi for the vehicle. It is assumed that the vehicle speed is known with an error of about 10 m/s, so that pre-compensation of the Doppler frequency shift is not perfect and a residual frequency offset is present in the received signal.

In mobile telecommunication systems, fixed reflecting obstacles at random positions with respect to the mobile phone generate constructive or destructive interference, which translates into variations of the received power as the user moves (fast or slow Rayleigh fading). In this case, this phenomenon is not present, since it is as if the reflecting surfaces generated by plasma were moving together with the vehicle: only a slowly varying multipath channel must be considered, the variations being due to the changed plasma conditions along the vehicle descent trajectory. The channel transfer function is assumed to be the same for the uplink and downlink, due to the reciprocity principle.

The processing capabilities of the ground station are not limited, and it is assumed that two parallel receivers are available, one for each of the two polarizations (right and left circular), and that a maximal ratio combiner is used to reduce the bit error rate. Each receiver performs frequency, phase, symbol synchronization, and equalization. The same type of complexity can be assumed for the IXV-like vehicle, while the ARD-like vehicles have only one receiver and cannot perform decoding. The Dynamic Link Budget Simulator allows for the simulation of different modulation and channel encoding schemes, so that it is possible to compare their performance and set the optimal relevant parameters. From the electric field values provided by AIPT at selected frequencies, DLBS evaluates (through interpolation) the channel transfer function in the frequency band necessary to correctly simulate the modulated signal. Moreover, DLBS interpolates in time between the "snapshots" analyzed by AIPT, so that each transmitted frame has a slightly different channel transfer function.

G. Results and conclusions

In the presence of plasma, the antenna radiation pattern undergoes both a shape distortion (power re-distribution), such as rippling effects, and a reduction on the total radiated power (due to cut-off rays). The extent of such effects depends on many factors: the vehicle shape, the plasma density distribution and the operative frequency.

Fig. 4 shows the temporal evolution of the IXV antenna gain, in the S band, within the critical region (where plasma is present). Correspondently to the lowest Mach numbers (15 and 17 which lead to lower plasma densities) the radiation pattern resembles very much that obtained in the free space condition. As the Mach number increases the radiation pattern becomes more and more distorted (Mach numbers equal to 25 and 27) due to the increased plasma density. As a consequence the link budget may degrade up to 20dB.

Increasing the operative frequency (e.g. switching from the S to the C band) may lead to a significant improvement of the overall performance as shown by Fig. 5**Errore. L'origine riferimento non è stata trovata.**, in which the radiation pattern, computed at 7.19 GHz, is much more similar to that in the free space condition. Therefore, losses are reduced of about 10dB.

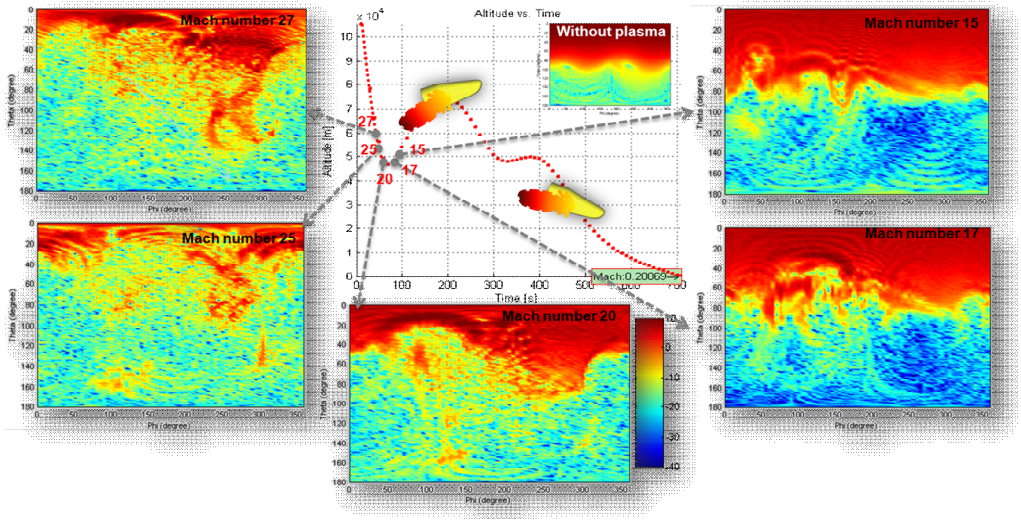

Fig. 4. Evolution of the IXV antenna gain in the critical region

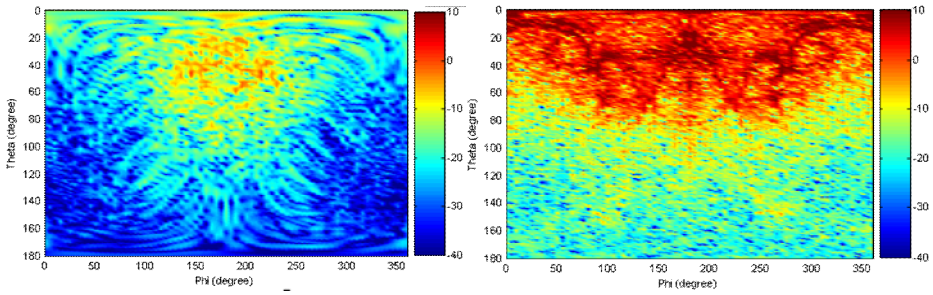

Fig. 5. Improvement of the ARD antenna radiation performance: gain at 2.26 GHz and 7.19GHz

For the case of IXV, Fig. 6 and 7 show, as examples, the transfer functions measured at the ground station (ship 1, at latitude -6.5 deg) assuming (a) antenna installed at side -Y onboard the vehicle transmitting in the S-band, (b) receiving antenna with both left and right hand circular polarizations, for the cases of Mach numbers 25 and 15. The frequency shown in the x-axis is actually the offset with respect to the center frequency 2.26 GHz. These transfer functions have been obtained as average over a cone with aperture 2 degrees around the ground station. Fig 8 shows instead the worst-case transfer function along the trajectory, which occurs at Mach number 25 at about 1 km to the South of the nominal ship position. It is possible to see that at Mach number 15, the LHCP Rx antenna receives most of the power and the transfer function is practically flat; on the contrary, for Mach number 25, a non-negligible fraction of power is received also on the RHC polarization and the transfer function is characterized by "holes" at some frequencies. Some of the holes are actually artifacts of interpolation, which can be removed by using AIPT with a smaller interval between two adjacent analyzed frequencies (the examples in this paper were obtained with a frequency spacing of 200 kHz). However strong attenuations really occur at some frequencies (as evaluated by AIPT , see Fig. 8). If the transmitted signal has a small bandwidth (as in the case of tele-command) and falls in one of these "holes", a communication blackout may occur due to reduction of the signal to noise ratio; if, on the contrary, the signal has a wide bandwidth, then the received power is sufficient but equalization becomes necessary.

For tele-command, it is convenient to widen the bandwidth of the transmitted signal by using a DSSS (Direct Sequence Spread Spectrum) technique; if a frequency synchronizer cannot be used at the receiver (ARD case), then 2FSK with incoherent reception is suggested, otherwise (IXV) 4PSK (Phase Shift Keying) or pre-coded GMSK (Gaussian Minimum Shift Keying) proved to be adequate. The CCSDS (Consultative Committee for

Eliminato: are actually

Eliminato: d

Space Data Systems) standard BCH(57,64) code [2] is suitable for tele-command in most cases. Starting and tail bits for tele-command word are not suitable to aid frequency synchronization and channel equalization, and a known preamble should be added to the transmitted frame.

For telemetry, it is not necessary to widen the bandwidth, but two receivers, one for each of the two polarizations, followed by a combiner, are suggested to improve the system performance, given the much smaller transmitted power. Frequency synchronization and channel equalization can be based on the use the synchronization marker standardized by CCSDS [3], but the longer synchronization marker is suggested (the one standardized for turbo codes with rate 1/6), even if it does not match the chosen encoding scheme. The suggested telemetry modulation is pre-coded GMSK [4], so that the signal is not distorted by the nonlinear amplifier onboard the vehicle; in some cases, however, distorted 4PSK, with larger bandwidth, has a better performance, results depending on the position of "holes" in the transfer function. Fig. 9 shows the power spectra of the transmitted and received signals for the worst-case channel of Fig. 8, assuming a GMSK transmitted signal with power 100 W; the effects of the large attenuation at center frequency can be noticed in the distortion of the scattering diagram. The equalizer, in this case, completely removes the inter-symbol interference and the resulting channel bit error rate is zero.

Turbo encoders with rate ½ or the concatenated Reed-Solomon (223,255) - rate ½ convolutional encoder [3] are both suitable for telemetry; it is not necessary to use more complex encoders with higher gains. In general, shorter frames are recommended, so that the channel estimation is more frequent at the receiver side.

Simultaneous transmission of telemetry from two antennas requires the use of a space-time encoding scheme, but a much more complex receiver is necessary. Space-time codes are easily used for channels with a flat transfer function (or which is constant in the subcarrier bandwidth as in OFDM), but in the presence of plasma equalization is necessary and the receiver becomes much more complex.

In the overall, plasma induces non-flat time-varying channel transfer functions, and the detrimental effects can be overcome by adopting the techniques currently used in mobile telecommunication systems.

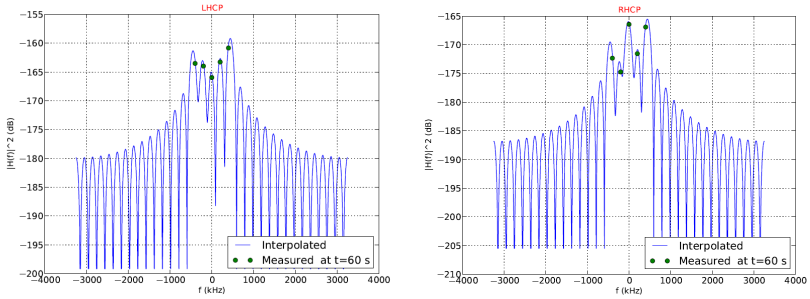

Fig. 6. Transfer functions for the LHCP and RHCP antennas at the G/S, case of Mach number 25, link IXV-ship 1

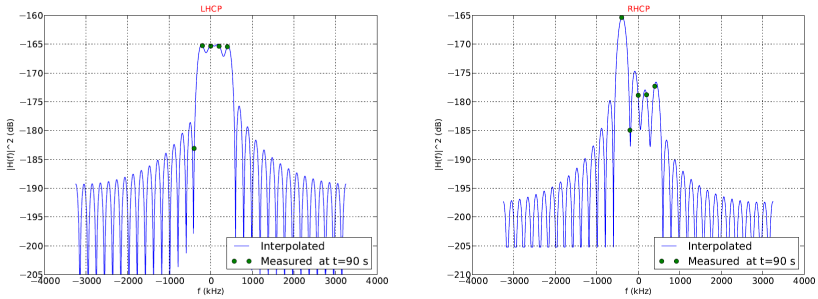

Fig. 7. Transfer functions for the LHCP and RHCP antennae at the G/S: case of Mach number 15, link IXV-ship 1

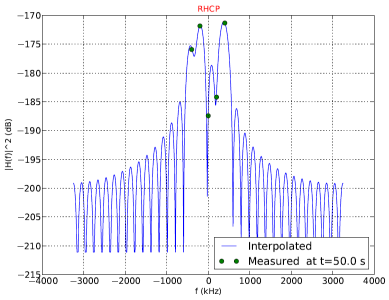

Fig. 8. Worst case transfer function for the link IXV-ship 1, RHC polarization.

Eliminato: 7

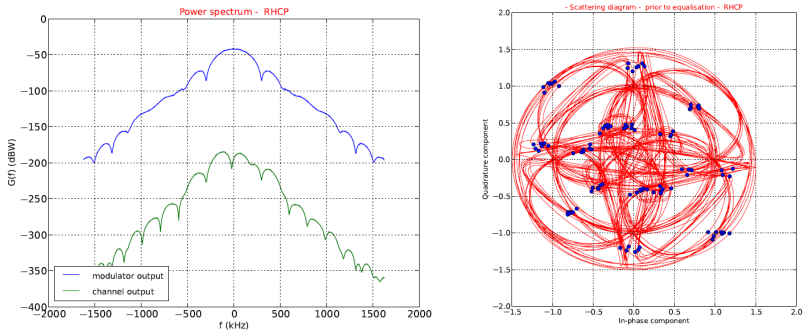

Fig. 9. Power spectrum of the transmitted and received telemetry signals, and scattering diagram of the received signal; information bit rate 192 kbit/s, transmitted power 100 W, GMSK modulation, turbo encoder with rate 1/2, channel of Fig. 8.

III. REFERENCES

[1] L. B. Felsen and N. Marcuvitz. *Radiation and Scattering of Waves*. Prentice-Hall, Englewood Cliffs, N. J., 1973.
[2] *CCSDS 201.0-B-3 Blue Book, Telecommand,* Part 1, Channel Service, June 2000
[3] *CCSDS 101.0-B-6 Blue Book, Telemetry Channel coding*, October 2002
[4] *CCSDS 413.0-G-2 Green Book, Bandwidth-Efficient Modulations, Summary of Definition, Implementation, and Performance,* October 2009